

Controllable Zinc Oxide Micro-Flowers Utilizing Pineapple Peel Extract

Ari Sulisty Rini^{1,*} , Rahmi Dewi¹ , Sri Hafiza Yanuar¹ , Yolanda Rati² , Yan Soerbakti¹ 

¹ Department of Physics, Universitas Riau, Simpang Baru 28293, Pekanbaru, Indonesia

² Department of Physics, Institut Teknologi Bandung, Ganesa 10 40132, Bandung, Indonesia

* Correspondence: ari.sulisty@lecturer.unri.ac.id;

Received: 20.05.2023; Accepted: 8.08.2023; Published: 25.11.2025

Abstract: Plant extract-based metal oxide production has been recognized as an environmentally benign alternative to replacing physical and chemical processes. Zinc oxide (ZnO) was created in this experiment by reacting a solution of zinc nitrate hexahydrate with pineapple peel extract. SEM photographs show the morphology of ZnO particles in the shape of spherical flowers with a particle size of 234nm. According to the X-ray diffraction pattern, the synthesized ZnO is a phase of the hexagonal wurtzite structure. In the UV-Vis spectrum, the maximum absorbance of ZnO occurs at 360nm with bandgap energy ranging from 3.18 to 3.30 eV. The absorption characteristic of crystalline ZnO is observed at a wavenumber of 464.23 cm⁻¹ based on the results of FTIR spectral analysis. Functional groups O–H, C–H, C=C, and C–O are also produced from secondary metabolites in pineapple peel extract. Due to the characteristics mentioned above, ZnO can be used as a photocatalyst and antibacterial material, offering an eco-friendly, cost-effective approach.

Keywords: absorption; antibacterial; crystalline; photocatalyst; wurtzite.

© 2025 by the authors. This article is an open-access article distributed under the terms and conditions of the Creative Commons Attribution (CC BY) license (<https://creativecommons.org/licenses/by/4.0/>), which permits unrestricted use, distribution, and reproduction in any medium, provided the original work is properly cited. The authors retain copyright of their work, and no permission is required from the authors or the publisher to reuse or distribute this article, as long as proper attribution is given to the original source.

1. Introduction

Metal oxide nanoparticles have been created in a variety of ways. However, the demand for ecologically friendly, simple, and cost-effective production has led to changes in the preparation process. Metal oxide nanoparticle production mediated by plant extracts and microorganisms has advanced considerably in recent years [1]. Green synthesis is the synthesis method included in this approach. This method is much safer than chemical and physical processes due to its simplicity and minimal use of harmful inorganic compounds [2]. Furthermore, because this method does not require high temperatures for nanoparticle synthesis, it is of great interest to researchers. Plant extracts are more commonly used in principle because they contain organic components such as enzymes, proteins, carbohydrates, and secondary metabolites, which are plentiful and easier to use than microbes [3]. Plant extracts perform as both reducing and directing agents for particle formation in particular orientations [4]. Plant extracts like *Sandoricum koetjape* peel [5], *Sambucus ebulus* leaves [1], *Andrographis paniculata* leaves [6], and *Deverratortuosa* [7] have been utilized in the production of nanoparticles.

Ananas comosus is the Latin name for the pineapple fruit. Riau Province is one of Indonesia's most productive pineapple-growing regions. Pineapple fruit is widely used in the food and beverage industries, generating thousands of tons of pineapple peel waste each year. Pineapple peel provides for around 37.1 % of the fruit's total weight. Pineapple peel contains 81% water, 20.87% crude fiber, 17.53% carbohydrates, 4.41% protein, and 13.65 % reducing sugar [8]. Secondary metabolites reported in pineapple peels include tannins, saponins, steroids, flavonoids, and phenols [9]. These substances serve as both reducing agents and stabilizers for metal nanoparticles and metal oxides.

Among various metal oxides, zinc oxide (ZnO) has a wide range of potential applications, including photovoltaics [10], water splitting [11], photocatalysis [12], and antibacterial agents [13]. ZnO is a semiconductor with a bandgap of 3.7 eV, is stable under UV radiation, and has high visible-light transparency [14]. Although there are several ways to produce ZnO, chemical methods have been found to contain hazardous chemicals [3]. Therefore, ZnO was prepared in this study using a synthetic green approach, with pineapple peel extract as the reducing agent. The results of characterization analysis using scanning electron microscopy (SEM), X-ray diffraction (XRD), UV-Vis spectroscopy, and Fourier transform infrared spectroscopy (FT-IR) reveal the physical properties of ZnO.

2. Materials and Methods

2.1. Preparation of pineapple peel extract.

The peels of pineapple fruit were collected and washed several times with distilled water to remove impurities. Then, the peel was dried, cut into small pieces, and ground into fine powder. As much as 1 g of powder is weighed and mixed with 100 mL of distilled water in a 200 mL glass beaker. The mixture was heated to 80°C for 60 minutes until the aqueous solution changed from watery to dark yellow, then filtered through Whatman No. 1 filter paper and stored at 4°C.

2.2. Synthesis of ZnO nanoparticles.

In 100 ml of pineapple peel extract, a 50mM zinc nitrate hexahydrate (ZNH) solution was mixed and stirred. A 5 M sodium hydroxide solution was added to achieve an alkaline pH, and the mixture was heated to 50°C until white precipitate formed. The precipitation was centrifuged at 4000 rpm and rinsed three times with sterile distilled water. ZnO samples were dried for a day at 110°C. The volume ratio of the extract and ZNH solution, namely 1:4, 1:1, and 4:1, was varied to synthesize ZnO nanoparticles.

2.3. Characterization technique.

SEM (HITACHI FLEXSEM 100), X-ray diffraction (Shimadzu XRD-7000 Maxima), UV-Vis spectroscopy (Analytic Jena, Specord 200 plus), and Fourier Transform Infrared Spectroscopy (Prestige 2100 Shimadzu) were used to investigate the surface morphology, structure, absorption, and functional bonding groups of the ZnO sample.

3. Results and Discussion

3.1. ZnO morphology.

The morphology of ZnO was examined by SEM at a magnification of 20,000 times, as shown in Figure 1. The morphology of ZnO particles was almost flower-like, with a spherical shape. Compared to the 1:1 and 1:4 samples, the 4:1 sample exhibits a more homogeneous particle structure because the nucleation process occurs more frequently [15]. Furthermore, in the ZnO synthesis process, the pineapple peel extract serves as both a reducing agent and a capping agent, producing uniform particle size and morphology [6]. This reveals that pineapple peel extract can be utilized to control particle size. ImageJ software was used to determine the diameter of the ZnO particles. The particle size depends on the ZNH solution composition and the volume of the extract. Sample 1:4 is the tiniest sample, with a size of 234.21 ± 35.23 nm. Meanwhile, the particle sizes of 1:1 and 4:1 samples are 327.53 ± 70.78 nm and 670.25 ± 53.77 nm, respectively.

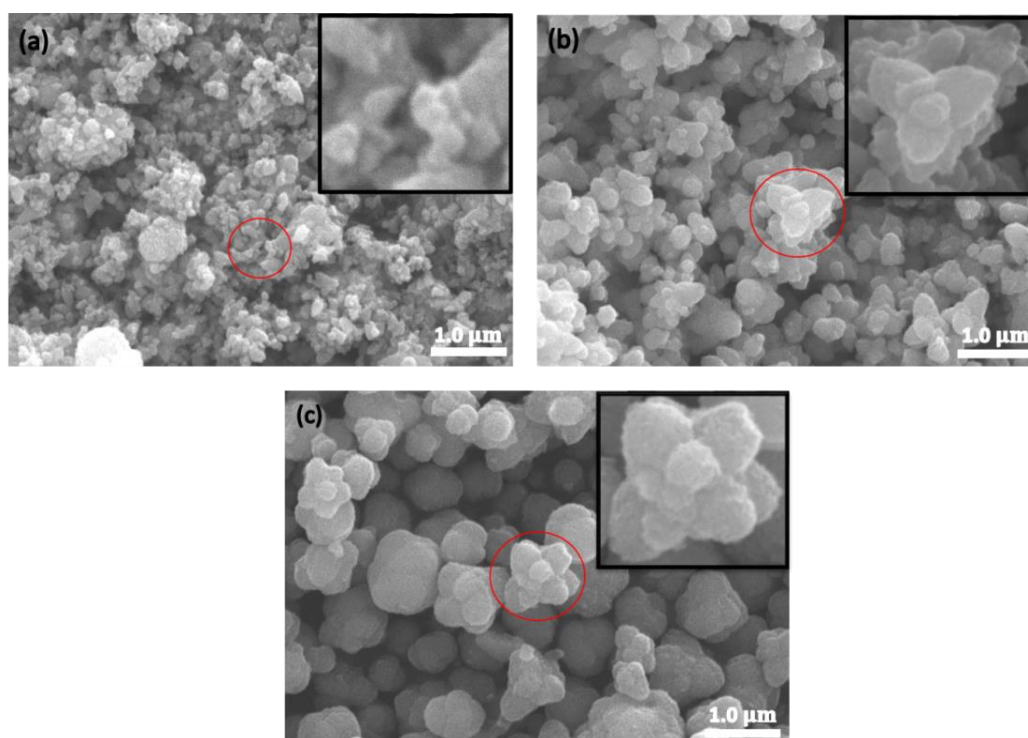


Figure 1. Morphological comparison of ZnO for sample volume ratio (a) 1:4; (b) 1:1; (c) 4:1.

3.2. XRD analysis.

The diffraction peaks (Figure 2) based XRD analysis of green synthesized ZnO using pineapple peel extract are at $2\theta = 31.64^\circ, 34.26^\circ, 36.12^\circ, 47.36^\circ, 56.44^\circ, 62.70^\circ,$ and 67.82° with hkl plane (100), (002), (101), (102), (110), (103), and (112). According to the data from the Joint Committee on Powder Diffraction Standard (JCPDS) No. 36-1451, ZnO has a hexagonal wurtzite crystal structure [16]. These results show that the ZnO sample obtained is pure and highly crystalline, with no other elemental crystalline phases or impurities present.

The highest diffraction peak was observed at $2\theta = 36.12^\circ$, corresponding to the (101) crystal plane. The full-width half maximum (FWHM) determined by fitting the Gaussian equation with the OriginPro 8.5.1 program is associated with the sharpness of the diffraction peak and the crystal size. With the crystal size of ZnO 13.28 nm, the lattice parameters achieved

are $a = 3.225 \text{ \AA}$ and $c = 5.221 \text{ \AA}$. These results align with those of Esakki *et al.* [15] obtained, considering lattice constants of $a = 3.22 \text{ \AA}$ and $c = 5.21 \text{ \AA}$.

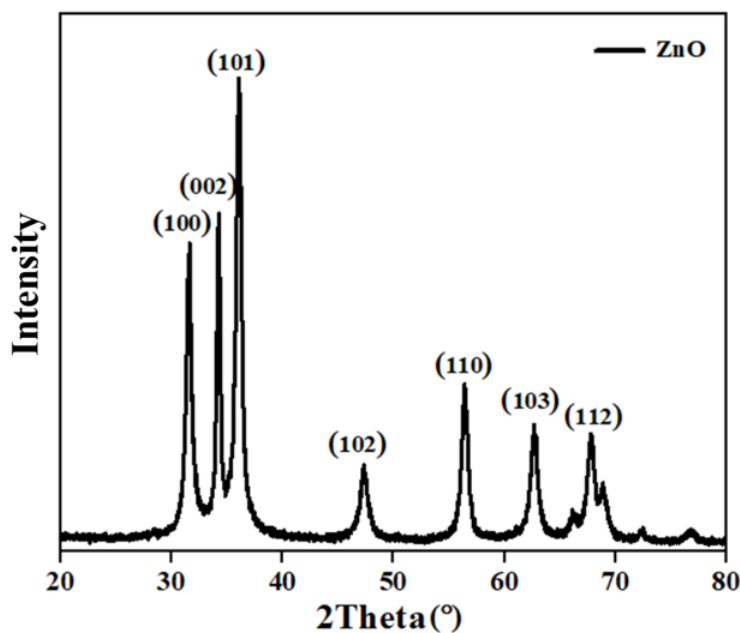


Figure 2. XRD pattern of ZnO.

3.3. Optical properties.

UV-Vis spectroscopy characterization aims to confirm the presence of nanoparticles produced and investigate ZnO's optical properties. The UV-Vis absorption spectrum of the ZnO sample can be seen in Figure 3 (a). All samples have absorbance peaks at a wavelength of $\sim 360 \text{ nm}$. ZnO nanoparticles exhibit characteristic absorption peaks below 400 nm [17]. A 1:4 sample owned the highest absorption peak, while the lowest was found in a 4:1 sample. This is because the 1:4 sample has a higher ZNH solution concentration than the other samples, resulting in stronger UV-Vis absorbance. According to the Lambert-Beer law, the concentration of the precursor material can increase the absorbance [18].

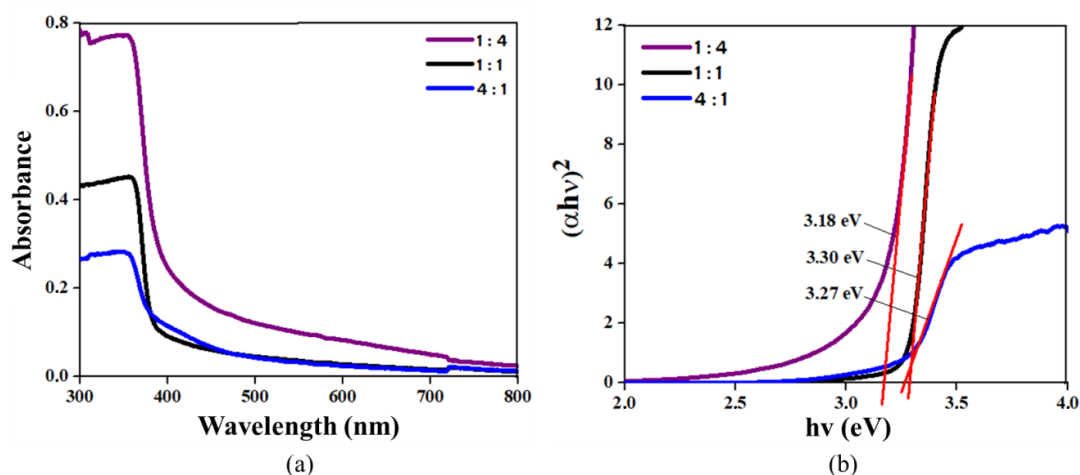


Figure 3. (a) Absorbance spectrum; (b) plot of $(\alpha h\nu)^2$ versus $h\nu$ of ZnO at various volume ratios of the extract and ZNH solution.

The UV-Vis spectrum contains information not only on light absorption but also on bandgap energy. The absorption coefficient at a given photon frequency, obtained by transforming the absorbance spectrum so that a graph of $(\alpha h\nu)^2$ versus $h\nu$ is obtained, has implications for the bandgap energy. Figure 3 (b) illustrates how the bandgap energy value was

estimated using a straight-line extrapolation technique to the X-axis from the graph. The bandgap energy of ZnO obtained is lower than that of ZnO synthesized using conventional methods (3.37 eV). This is due to an internal force that is strong enough to affect the energy bandgap [19]. The narrower the distance between the valence band and the conduction band, the smaller the band gap energy value of a material. Therefore, the energy required to excite electrons when irradiated by photons is small, resulting in strong light absorption. This property makes the green synthesized ZnO potentially applicable as a photocatalyst.

3.4. Functional group analysis.

The functional groups and categories of compounds present in the sample ZnO were evaluated using FTIR spectroscopy. The O-H functional group represented the widest absorption in the 3000 cm⁻¹ to 3700 cm⁻¹ area in the FTIR spectrum (Figure 4). The absorption of the carboxylic acid functional group (C=O) was confirmed at 1744.48 cm⁻¹ in the pineapple peel extract, as shown in Figure 4(a). Still, no such functional group was observed upon the addition of ZNH solution [20]. At a wavenumber of 464.23 cm⁻¹, the wave absorption of crystalline ZnO can be observed, as shown in Figure 4(b).

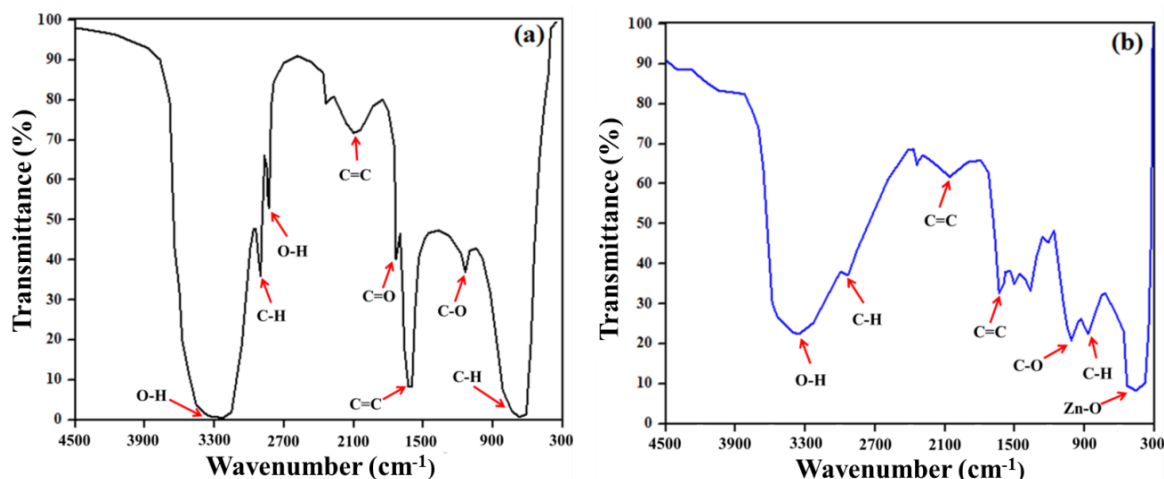


Figure 4. FT-IR spectrum of (a) pineapple peel extract; (b) pineapple peel extract + ZNH solution.

Table 1 shows the functional groups and wavenumbers for each sample. Based on the FT-IR spectrum, there is a slight shift in the wavenumbers of the same functional groups. The functional groups that bind to the surface of the ZnO particles stabilize during the Zn²⁺ reduction process to Zn⁰, causing this shift [1]. The weakening of chemical bonds causes several functional groups that aren't apparent in the ZnO sample. The bond is broken because the solution is heated for a long time during the synthesis process [6].

Table 1. The functional groups of pineapple peel extract and ZnO.

Functional group	Wavenumber (cm ⁻¹)	
	Pineapple peel extract	ZnO
O-H (phenol)	3300.93	3392.37
C-H (aromatic)	2915.55	2940.75
O-H (phenol)	2832.50	-
C=C (aromatic)	2079.47	2062.67
C=C (carboxylic acid)	1744.48	-
C=C (aromatic)	1619.44	1626.91
C-O (eter, ester)	1141.68	1016.64
C-H (aromatic)	690.05	865.47
ZnO crystals	-	464.23

4. Conclusions

Based on the results of the analyzed research, it can be concluded that adding pineapple peel extract results in a more homogeneous, flower-like morphology due to faster reduction. Synthesized ZnO green obtained a hexagonal wurtzite crystal size of 13.28nm. The greater the volume of the ZNH solution, the greater the UV-Vis absorbance. The characteristics of ZnO based on the FTIR spectrum were obtained at a wave number of 464.23cm^{-1} . Therefore, ZnO synthesized using a simple method from pineapple peel extract can be used as a photocatalyst and antibacterial material.

Author Contributions

Conceptualization, A.S.R. and R.D.; methodology, A.S.R. and S.H.Y.; software, S.H.Y. and Y.R.; validation, A.S.R. and R.D.; formal analysis, A.S.R., S.H.Y., and Y.R.; investigation, A.S.R. and R.D.; data curation, S.H.Y., Y.R., and Y.S.; writing—original draft preparation, S.H.Y., Y.R., and Y.S.; writing—review and editing, Y.R. and Y.S. All authors have read and agreed to the published version of the manuscript.

Institutional Review Board Statement

Not applicable.

Informed Consent Statement

Not applicable.

Data Availability Statement

Data supporting the findings of this study are available upon reasonable request from the corresponding author.

Funding

This research received no external funding.

Acknowledgments

We thank the Riau University Research and Community Service Institute for supporting this research.

Conflicts of Interest

The authors declare no conflict of interest.

References

1. Alamdari, S.; Ghamsari, M.S.; Lee, C.; Han, W.; Park, H.-H.; Tafreshi, M.J.; Afarideh, H.; Ara, M.H.M. Preparation and characterization of zinc oxide nanoparticles using leaf extract of *Sambucus ebulus*. *Appl. Sci.* **2020**, *10*, 4620, <https://doi.org/10.3390/app10103620>.
2. Alprol, A.E.; Mansour, A.T.; El-Beltagi, H.S.; Ashour, M. Algal extracts for green synthesis of zinc oxide nanoparticles: Promising approach for algae bioremediation. *Materials* **2023**, *16*, 2819, <https://doi.org/10.3390/ma16072819>.

3. Ahmed, S.F.; Mofijur, M.; Rafa, N.; Chowdhury, A.T.; Chowdhury, S.; Nahrin, M.; Saiful Islam, A.B.M.; Ong, H.C. Green approaches in synthesising nanomaterials for environmental nanobioremediation: Technological advancements, applications, benefits and challenges. *Environ. Res.* **2022**, *204*, 111967, <https://doi.org/10.1016/j.envres.2021.111967>.
4. Rini, A.S.; Rati, Y.; Fadillah, R.; Farma, R.; Umar, L.; Soerbakti, Y. Improved photocatalytic activity of ZnO film prepared via green synthesis method using red watermelon rind extract. *Evergreen* **2022**, *9*, 1046–1055, <https://doi.org/10.5109/6625718>.
5. Rini, A.S.; Fitriasia, A.; Rati, Y.; Umar, L.; Soerbakti, Y. Bio-colloidal silver nanoparticles prepared via green synthesis using *Sandoricum koetjape* peel extract for selective colorimetry-based mercury ions detection. *Karbala Int. J. Mod. Sci.* **2023**, *9*, 12, <https://doi.org/10.33640/2405-609X.3299>.
6. Muthulakshmi, V.; Kumar, P.; Sundarajan, M. Green synthesis of ionic liquid mediated ytterbium oxide nanoparticles by *Andrographis paniculata* leaves extract for structural, morphological and biomedical applications. *J. Environ. Chem. Eng.* **2021**, *9*, 105270, <https://doi.org/10.1016/j.jece.2021.105270>.
7. Selim, Y.A.; Azb, M.A.; Ragab, I.; Abd El-Azim, M.H.M. Green synthesis of zinc oxide nanoparticles using aqueous extract of *Deverra tortuosa* and their cytotoxic activities. *Sci. Rep.* **2020**, *10*, 3445, <https://doi.org/10.1038/s41598-020-60541-1>.
8. Hatam, S.F.; Suryanto, E.; Abidjulu, J. Aktivitas antioksidan dari ekstrak kulit nanas (*Ananas comosus* (L) Merr). *Pharmakon* **2013**, *2*.
9. Azizan, A.; Lee, A.X.; Hamid, N.A.A.; Maulidiani, M.; Mediani, A.; Ghafar, S.Z.A.; Zolkeflee, N.K.Z.; Abas, F. potentially bioactive metabolites from pineapple waste extracts and their antioxidant and α -glucosidase inhibitory activities by ^1H NMR. *Foods* **2020**, *9*, 173, <https://doi.org/10.3390/foods9020173>.
10. Tarasenko, N.; Shustava, E.; Butsen, A.; Kuchmizhak, A.A.; Pashayan, S.; Kulinich, S.A.; Tarasenko, N. Laser-assisted fabrication and modification of copper and zinc oxide nanostructures in liquids for photovoltaic applications. *Appl. Surf. Sci.* **2021**, *554*, 149570, <https://doi.org/10.1016/j.apsusc.2021.149570>.
11. Kegel, J.; Povey, I.M.; Pemble, M.E. Zinc oxide for solar water splitting: A brief review of the material's challenges and associated opportunities. *Nano Energy* **2018**, *54*, 409–428, <https://doi.org/10.1016/j.nanoen.2018.10.043>.
12. Abdullah, F.H.; Abu Bakar, N.H.H.; Bakar, M.A. Low temperature biosynthesis of crystalline zinc oxide nanoparticles from *Musa acuminata* peel extract for visible-light degradation of methylene blue. *Optik* **2020**, *206*, 164279, <https://doi.org/10.1016/j.ijleo.2020.164279>.
13. Kalpana, V.N.; Kataru, B.A.S.; Sravani, N.; Vigneshwari, T.; Panneerselvam, A.; Rajeswari, V.D. Biosynthesis of zinc oxide nanoparticles using culture filtrates of *Aspergillus niger*: Antimicrobial textiles and dye degradation studies. *OpenNano* **2018**, *3*, 48–55, <https://doi.org/10.1016/j.onano.2018.06.001>.
14. Jeong, J.H.; Park, S.; Kim, B.J.; Heo, S.B.; Kim, T.Y.; Shin, J.S.; Yu, J.H.; Ma, J.H.; Kim, M.G.; Kang, S.J. Improving the visible-light photoresponse characteristics of a ZnO phototransistor via solution processable Li dopants. *J. Mater. Chem. C* **2021**, *9*, 9650–9658, <https://doi.org/10.1039/D1TC02088A>.
15. Esakki, E.S.; Deepa, G.; Vivek, P.; Devi, L.R.; Sheeba, N.L.; Sundar, S.M. Investigation on electrochemical analysis of ZnO nanoparticles and its performance for dye-sensitized solar cells using various natural dyes. *J. Indian Chem. Soc.* **2023**, *100*, 100889, <https://doi.org/10.1016/j.jics.2023.100889>.
16. Demissie, M.G.; Sabir, F.K.; Edossa, G.D.; Gonfa, B.A. Synthesis of zinc oxide nanoparticles using leaf extract of *Lippia adoensis* (koseret) and evaluation of its antibacterial activity. *J. Chem.* **2020**, *2020*, 7459042, <https://doi.org/10.1155/2020/7459042>.
17. Melnyk, Y.; Starchevskiy, R.; Melnyk, S. Transesterification of sunflower oil triglycerides by 1-butanol in the presence of d-metal oxides. *Vopr. Khimii Khimicheskoi Tekhnologii* **2019**, *4*, 95–100, <https://doi.org/10.32434/0321-4095-2019-125-4-95-100>.
18. Dimitrov, T.I.; Ibrevva, T.H.; Zaichuk, A.V.; Markovska, I.G.; Amelina, A.A.; Karasik, E.V. Synthesis and study of low-temperature ferrum-willemite ceramic pigments. *Vopr. Khimii Khimicheskoi Tekhnologii* **2019**, *6*, 69–73, <https://doi.org/10.32434/0321-4095-2019-127-6-69-73>.
19. Saber, O.; Shaalan, N.M.; Ahmed, F.; Kumar, S.; Alshoabi, A. One-step multi-doping process for producing effective zinc oxide nanofibers to remove industrial pollutants using sunlight. *Crystals* **2021**, *11*, 1268, <https://doi.org/10.3390/cryst11101268>.
20. Danjuma, M.S.; Adamu, A.; Kumar, S.A.; Umar Kura, N. Eco-friendly synthesis and characterization of iron nanoparticles using crude extract from *Eucalyptus globulus* leaves as reducing and capping agents. *Nanochem. Res.* **2022**, *7*, 135–142, <https://doi.org/10.22036/ncr.2022.02.008>.

Publisher's Note & Disclaimer

The statements, opinions, and data presented in this publication are solely those of the individual author(s) and contributor(s) and do not necessarily reflect the views of the publisher and/or the editor(s). The publisher and/or the editor(s) disclaim any responsibility for the accuracy, completeness, or reliability of the content. Neither the publisher nor the editor(s) assume any legal liability for any errors, omissions, or consequences arising from the use of the information presented in this publication. Furthermore, the publisher and/or the editor(s) disclaim any liability for any injury, damage, or loss to persons or property that may result from the use of any ideas, methods, instructions, or products mentioned in the content. Readers are encouraged to independently verify any information before relying on it, and the publisher assumes no responsibility for any consequences arising from the use of materials contained in this publication.